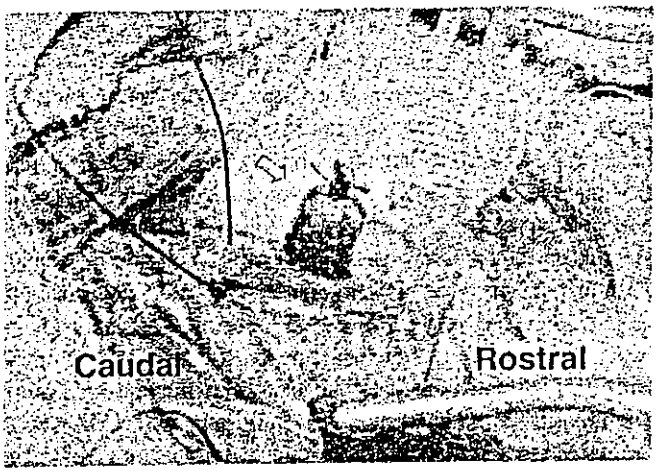

Fig. 2. Preparation of an experimental extracranial carotid artery aneurysm in dogs. A cervical lateral-wall carotid artery aneurysm is made with the external jugular vein of one side. The vein patch is anastomosed end-to-side to the carotid artery under microscopy.

inserted into the femoral artery and placed. A 5 French PTA balloon catheter with a stent graft was inserted through the sheath and advanced across the neck of the aneurysm under fluoroscopy. The balloon was inflated, and the stent graft was released. Angiography was performed before and after stent graft using a C-arm image intensifier with a neurovascular software supplement (Series 9000; OEC-Diasonics, Cathex, Japan). After implantation on both sides, the balloon catheter was removed, and the femoral artery was ligated.

2.4. Histologic process and photography

Follow-up angiography was performed prior to sacrifice at 1 week, 1 month and 3 months after stenting. All aneurysms and adjacent segments of the carotid arteries were removed and fixed in a 10% solution of phosphate-buffered formaldehyde. Specimens were embedded in methylmethacrylate. For light microscopic study, longitudinal sections 0.5 mm thick were obtained by means of a circular diamond saw and were hand-polished to a thickness of 30–40 μm. After the specimens were processed and embedded, the paraffin blocks were cut into sections approximately 5 μm thick, which was stained with hematoxylin–eosin and/or Masson's trichrome stain. A part of each specimen was processed for scanning electron microscopy.

3. Results

3.1. Prepared stent graft

The fabricated stent graft was easily mounted on a PTA balloon and was expanded smoothly (Fig. 1).

3.2. Surgery

Aneurysms were successfully constructed on both carotids in all animals, except for one aneurysm. All animals recovered from surgery within 4 h and were used for the current study.

3.3. Angiographic findings

Immediately after embolization, inflow into the aneurysm was almost terminated. In a few minutes, all aneurysms became invisible by angiography. At 1 week, 1 month (Fig. 3) and 3 months after embolization, none of the aneurysms could be identified on angiograms with enough patent parent arteries.

3.4. Gross observations

Immediately after embolization, the aneurysms occluded by stent grafts were thrombosed on external appearance. At 1 week, 1 month and 3 months, the aneurysms were thrombosed and firm on outward appearance. Sagittal sections of specimens showed thin intima ingrowth via or along the micropores of the stent graft in the neck of the occluded aneurysms, even at 1 week after embolization, with no entry to the aneurysms at any stages.

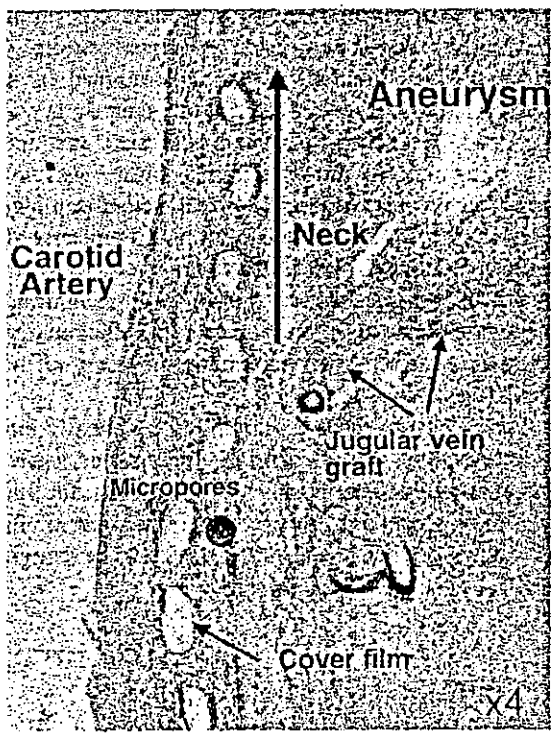

Fig. 3. Aneurysm, 1 week after stent graft placement H & E stain. This sagittal section shows a caudal part of the embolized aneurysm. The aneurysm is completely packed with old thrombi with enough patent parent artery. There is intimal ingrowth through the micropores into the luminal surface and the aneurysm cavity. The aneurysm is completely occluded by a combination of mechanical stent graft and biological intimal barrier.

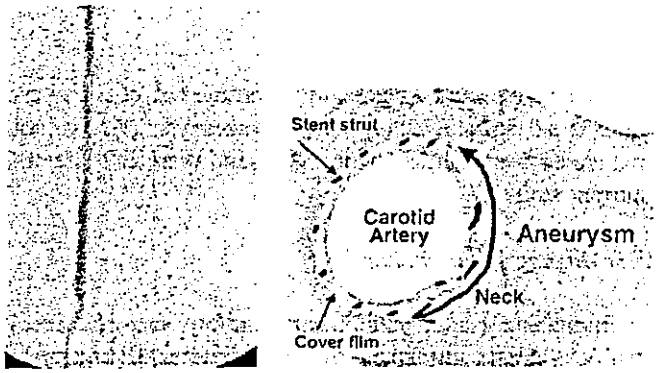

Fig. 4. Microscopic section, 1 month after stent graft placement. (a) Carotid angiogram shows complete occlusion of the aneurysm with enough patent carotid artery. (b) Low-power cross-section photomicrograph of the aneurysm treated with our stent graft, harvested 1 month after implantation (Masson's trichrome stain). There is organized thrombus formation within the aneurysm and mild intimal fibrocellular proliferation of the parent vessel wall. There is the neck of the aneurysm (a curved arrow) corresponding to the arterial wall defect at the site of anastomosis with the external jugular vein.

3.5. Histopathologic findings

Light microscopy of the specimens removed immediately after implantation revealed that the neck of the aneurysm was closed by the stent graft, and that the aneurysm was also completely packed with thrombi. At 7 days after implantation, thrombi occupying each aneurysm cavity were observed. A thin layer of neointima promoted by tissue ingrowth via micropores covered the in-stent lumen in the early period. The luminal surface of the stent was smooth. SEM findings showed that the luminal surface was covered with confluent endothelial cells. In all stented samples, the aneurysms were filled with mature fibrous connective tissue (organized thrombus). Within the fibrous connective tissue (deep to the organized mural thrombus or neointima surrounding the stent struts), there was mild inflammatory cell infiltration consisting of macrophages, many of which contained hemosiderin.

In specimens obtained 1 month (Fig. 4) and 3 months after embolization, an intensive granulomatous tissue proliferation was observed. In all stented arteries, the luminal surface of the stent was covered by a thin layer of fibrous tissue and endothelial cells. This tissue layer completely covered the neck of the aneurysm.

4. Discussion

Our developed stent graft showed early complete occlusion of experimental aneurysms without early thrombotic occlusion of the parent carotid artery and with late-term full patency. This graft has been developed for treatment of arterial stenosis. It consists of a balloon expandable stent with a thin SPU film, onto which micropores were placed by an excimer laser ablation technique [7] and heparin was impregnated by photoreactive gelatination [6].

Intravascular surgery for intracranial aneurysms is becoming an attractive alternative to conventional surgery, especially after the introduction of GDC electrolytically detachable coils [10,11]. However, coils do not always fill the aneurysm cavity completely, and additional thrombus formation is necessary to achieve total angiographic occlusion of the aneurysm. Incomplete healing of aneurysms with recurrences following coil embolization in dogs and rabbits was explained by deficient neointima formation. Endothelialization of the coils may be useful in preventing thromboembolic complications. Coils modified with collagen or other growth factors that stimulate fibrosis may have the potential to provide a better framework for fibroblast migration and endothelial cell formation [12].

Promotion of thicker, stronger neointima leads to more complete or permanent obliteration of aneurysms following embolization [9]. However, coil embolization of aneurysms has several disadvantages. First, there is a risk of intraoperative bleeding because of overdistension. Secondly, there is a risk of rebleeding from the remaining aneurysm because of incomplete occlusion of the neck [3,13]. Thirdly, there is a risk of recirculation because of coil compaction.

To avoid these limitations of coil embolization, endovascular balloon expandable [14] or self-expanding [15,16] stenting of experimental aneurysms has been reported to be promising. Stenting with a tubular self-expanding porous stent achieved complete and selective occlusion of the aneurysm without penetrating the aneurysmal sac. The endovascular prosthesis, by bridging the aneurysm neck, directs the blood toward the distal part of the parent vessel, which reduces the inflow into the aneurysm (blood diversion or channeling effect) and finally promotes occlusion of the aneurysm [17]. Blood stasis after deployment of a stent leads to thrombus formation, fibrotic growth and eventually thrombus organization, resulting in ablation of the residual aneurysmal lumen. In the case of broad neck aneurysm, an uncovered stent serves as an endoluminal scaffold for coils, preventing coil herniation into the parent artery and decreasing incomplete thrombotic occlusion of the aneurysm [18,19]. Bared stents do not cause acute exclusion of the aneurysmal lumen from the native vessel lumen. Ideally, stent grafts would be used to exclude aneurysms immediately. There have been reports on the use of stent grafts to exclude broad neck aneurysms or fistulas from their circulation. A stent graft may be able to close a large orifice and immediately halt blood flow into the aneurysm. The rationale for our technique is that by isolating a segment of the artery, the likelihood that intimal hyperplasia will intervene to produce restenosis is reduced.

Our developed stent graft showed almost instant occlusion of the aneurysm after deployment and lessened the risk of embolic events due to continuous washout of produced thrombus. A thin layer of neointima promoted by tissue

ingrowth via micropores covered the in-stent lumen in the early period after placement. In our study, the neck was covered with an endothelial layer as early as 7 days after placement. Restoration of the endothelium inhibits smooth muscle cell accumulation after denuding arterial injury [20] and stimulation of endothelial restoration simultaneously maximizes regression of intimal hyperplasia [21]. At 1 month and 3 months after occlusion of the aneurysms by stent graft implantation, histopathologic study revealed mature fibrous connective tissue and collagen, indicating a well-organized thrombus filling each aneurysmal lumen, and satisfactory patency of the parent carotid artery.

Our developed stent graft might be considered as a promising material for embolization of extracranial aneurysms, not only in animal models, but also in humans.

References

[1] Kuether TA, Nesbit GM, Barnwell SL. Clinical and angiographical outcomes, with treatment data, for patients with cerebral aneurysms treated with Guglielmi detachable coils: a single center experience. Neurosurgery 1998;43:1016–23.

[2] Bristra EH, Rinkel GJE, Graaf Y, Rooij WJJ, Algra A. Treatment of intracranial aneurysms by embolization with coils. A systematic review. Stroke 1999;30:470–6.

[3] Byrne JV, Sohn M, Molyneux AJ. Five-year experience in using coil embolization for ruptured intracranial aneurysms: outcomes and incidence of late bleeding. J Neurosurg 1999;90:656–63.

[4] Moret J, Cognard C, Weil A, Castaings L, Rey A. Reconstruction technique in the treatment of wide-neck intracranial aneurysms: long-term angiographic and clinical results —Apropos of 56 cases. J Neuroradiol 1997;24:30–44.

[5] Kerber AV, Buschman RW. Experimental carotid aneurysms: I. Simple surgical production and radiographic evaluation. Invest Radiol 1976;12:154–7.

[6] Matsuda T, Nakayama Y. Surface microarchitectual design in biomedical application: in vitro transmural endothelialization on microporous segmented polyurethane films fabricated using an excimer laser. J Biomed Mater Res 1996;31:235–42.

[7] Doi K, Nakayama Y, Matsuda T. Novel compliant and tissue-permeable microporous polyurethane vascular prosthesis fabricated using an excimer laser ablation technique. J Biomed Mater Res 1996;31:27–33.

[8] German WJ, Black SPW. Experimental production of carotid aneurysms. N Engl J Med 1954;250:104–6.

[9] Raymond J, Venne D, Allas S, Roy D, Oliva VL, Denbow N, Salazkin I, Leclerc G. Healing mechanisms in experimental aneurysms: I. Vascular smooth muscle cells and neointima formation. J Neuroradiol 1999;26:7–20.

[10] Guglielmi G, Vinuela F, Dion J, Duckwiler G. Electrothrombosis of saccular aneurysms via endovascular approach: Part 2. Preliminary clinical experience. J Neurosurg 1991;75:8–14.

[11] Vinuela F, Duckwiler G, Mawad M. Guglielmi detachable coil embolization of acute intracranial aneurysms: perioperative anatomical and clinical outcome in 403 patients. J Neurosurg 1997;86:475–82.

[12] Abrahams JM, Diamond SL, Hurst RW, Zager EL, Grady MS. Topic review: surface modifications enhancing biological activity of Guglielmi detachable coils in treating intracranial aneurysms. Surg Neurol 2000;54:34–41.

[13] Raymond J, Roy D. Safety and efficacy of endovascular treatment of acutely ruptured aneurysms. Neurosurgery 1997;41(6):1235–45.

[14] Turjman F, Acevedo G, Moll T, Duquensnel J, Eloy R, Sindou M. Treatment of experimental carotid aneurysms by endoprosthesis implantation: preliminary report. Neurol Res 1993;15:181–4.

[15] Geremia G, Haklin M, Brennecke L. Embolization of experimentally created aneurysms with intravascular stent devices. AJNR, Am J Neuroradiol 1994;15:1223–31.

[16] Geremia G, Brack T, Brennecke L, Haklin M, Falte R. Occlusion of experimentally created fusiform aneurysms with porous metallic stents. AJNR, Am J Neuroradiol 2000;21:739–45.

[17] Wakhloo Ajay K, Schellhammer F, Vries de J, Haberstroh J, Schumacher M. Self-expanding and balloon-expandable stents in the treatment of carotid aneurysms: an experimental study in a canine model. AJNR, Am J Neuroradiol 1994;15:493–502.

[18] Turjma F, Massoud TF, Ji C, Guglielmi G, Vinuela F, Robert J. Combined stent implantation and endosaccular coil placement for treatment of experimental wide-necked aneurysms: a feasibility study in swine. AJNR, Am J Neuroradiol 1994;15:1087–90.

[19] Szikora I, Geterman LR, Wells KM, Hopkins LN. Combined use of stent and coils to treat experimental wide-necked carotid aneurysms; preliminary results. AJNR, Am J Neuroradiol 1994;15:1091–102.

[20] Schwartz SM, Stemerman MB, Benditt EP. The aortic intima: II. Repair of the aortic lining after mechanical denudation. Am J Pathol 1975;81:15–42.

[21] Bjornsson TD, Dryjski M, Tluczek J, Mennie R, Ronan J, Mellin TN, Thomas KA. Acidic fibroblast growth factor promotes vascular repair. Proc Natl Acad Sci USA 1991;88:8651–5.

OCCLUSION OF EXPERIMENTAL ANEURYSMS WITH HEPARIN-LOADED, MICROPOROUS STENT GRAFTS

Shogo Nishi, M.D.
Department of Neurosurgery, Takatsuki Red Cross Hospital, Osaka, Japan

Yasuhide Nakayama, Ph.D.
Department of Bioengineering, National Cardiovascular Center Research Institute, Osaka, Japan

Hatsue Ishibashi-Ueda, M.D.
Department of Pathology, National Cardiovascular Center Hospital, Osaka, Japan

Takehisa Matsuda, Ph.D.
Department of Biomedical Engineering, Graduate School of Medicine, Kyushu University, Fukuoka, Japan

Reprint requests:
Shogo Nishi, M.D., Department of Neurosurgery, Takatsuki Red Cross Hospital, 1-1-1 Abuno, Takatsuki City, Osaka 569-1096, Japan.
Email: sn1957@ja3.so-net.ne.jp

Received, November 5, 2002.
Accepted, August 12, 2003.

OBJECTIVE: An embolization technique using a stent graft has been developed to replace the conventional type of direct surgery or neurointervention with platinum coils and/or bare stents. The utility of a commercially available metal stent wrapped with a microporous elastomeric film coated with a thin, heparin-loaded, photocured gelatinous layer for the treatment of experimental carotid artery sidewall aneurysms in dogs was evaluated.

METHODS: The stent graft was used for embolization of experimental carotid artery aneurysms in dogs. The aneurysms were prepared bilaterally in canine carotid arteries with branching of an external jugular vein patch.

RESULTS: The entries into all of the aneurysms were occluded immediately after placement of the stent grafts, and the aneurysms were embolized by thrombus formation even 1 week after deployment. All of the parent carotid arteries in which stent grafts were placed were patent, without severe stenosis, immediately (n = 2), 1 week (n = 4), 1 month (n = 3), and 3 months (n = 4) after placement. Scanning electron microscopy demonstrated that the luminal surfaces of the stent grafts were entirely endothelialized as soon as 1 week after placement, via transmural tissue ingrowth through the micropores formed in the covering film.

CONCLUSION: The stent graft we have developed seems to be highly promising for the treatment of aneurysms, especially with respect to immediate termination of blood inflow for aneurysm occlusion and rapid endothelialization in the aneurysm neck.

KEY WORDS: Aneurysm, Covered stent, Dog, Heparin coating, Microporous, Stent graft

Neurosurgery 53:1397-1405, 2003 DOI: 10.1227/01.NEU.0000093427.89827.12 www.neurosurgery-online.com

The improvement of endovascular techniques for the treatment of intracranial aneurysms with Guglielmi electrolytically detachable coils has led to excellent clinical results (5, 6, 21). However, intrinsic technical problems remain, especially with the occlusion of surgically difficult large or giant aneurysms, for which 20 to 30 coils may be needed for complete occlusion (23). In addition, treatment of such broad-based aneurysms may cause occlusion of the parent vessel with the entry of misplaced occlusive material. Thromboembolic complications may also occur, and neck remnants may cause regrowth and rupture of the aneurysm. In addition, placement of a microcatheter in the aneurysm carries a risk of rupture and dislodgement of the thrombus. An embolization technique using a simple stent covered with nonporous polymeric film has been investigated as a novel approach for the treatment of extracranial aneurysms. The endovascular technique has several advantages over direct surgery for the treatment of intracranial or extracranial aneurysms. For example, the aneurysm neck can be completely occluded with a physical barrier bearing a covering film. Simple covered stents have been experimentally applied for percutaneous transluminal angioplasty (PTA) of coronary arteries. The materials used in those studies were degradable polymers such as poly(glycolic acid) (17) or poly(lactic acid) (17, 31, 37) or nondegradable polymers such as polyurethane (18, 34), silicone (27), or polyester (7). However, it was reported that stents covered with nonporous polymer films implanted in swine coronary arteries caused significant inflammation, thrombus formation, and excessive growth of vascular smooth muscle cells (VSMCs), result-

ing in severe stenosis (29, 30). Those findings were attributable to the fact that covering films greatly increase the blood-contact surface area, in comparison with uncovered stents, eventually increasing the frequency of thrombus formation and inflammation.

Recently, we designed a novel stent graft that physically controls tissue ingrowth and can carry an immobilized drug for treatment of arterial stenosis. The graft consists of a balloon-expandable metal stent and a chemically modified microporous elastomeric film, which can act as a drug reservoir. Thrombus formation leading to occlusion at an early stage after implantation is prevented by a heparin-loaded gelatinous coating on the film surface. Rapid induction of intraluminal endothelialization and control of tissue ingrowth through the micropores from surrounding tissues were experimentally achieved. In this study, we investigated the utility of a commercially available metal stent wrapped with a microporous elastomeric film coated with a thin, heparin-loaded, photocured gelatinous layer for the treatment of experimental carotid artery sidewall aneurysms in a canine model.

MATERIALS AND METHODS

We created 13 experimental saccular aneurysms (19) in seven adult mongrel dogs weighing 13 to 15 kg. The aneurysms were 0.5 cm in diameter at the neck and 1.0 cm in length. The high-performance stent grafts were metal stents (Palmaz stents; Cordis, Johnson & Johnson, Tokyo, Japan) bearing a thin, microporous, segmented polyurethane (SPU) film impregnated with heparin (22). The grafts were placed in the common carotid artery, across the aneurysms on both sides. Aspirin and ticlopidine were administered orally at daily doses of 81 mg and 100 mg, respectively, beginning 1 week before embolization of the aneurysms. Angiography was performed before stent graft placement, immediately after stent graft deployment, and 1, 4, and 12 weeks after stenting, followed by sampling.

Fabrication of Stent Grafts

Micropores were formed in a commercially available SPU film (thickness, 30 μm; Sheedom Co., Tokyo, Japan) with an excimer laser ablation technique (9). The pore size was 100 μm, and the interpore distance was 250 μm. After formation of the micropores, 1 mg (164.5 units)/cm^2 heparin was immobilized onto the surface of the film with 20 mg/cm^2 photoreactive gelatin (23) (*Figs.* 1 and 2). With the aid of a microscope, the modified thin SPU film was sutured onto the strut of a stent (Palmaz stent) with 10-0 nylon thread, rolled, and fixed to the stent with *N,N*-dimethylformamide (*Fig.* 2). Before use, the fabricated stent grafts were sterilized in a bath of 0.5% Maskin alcohol, irrigated with saline solution, and firmly mounted on PTA balloons (5-French Power Flex PTA balloons; Cordis, Johnson & Johnson).

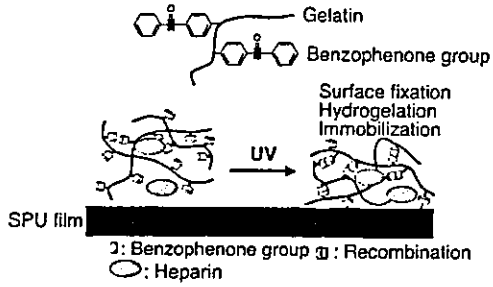

FIGURE 1. *Diagram of heparin immobilization on the covering film surface. Surface hydrogelation with ultraviolet photo-cross-linking of benzophenone-derivatized gelatin causes entrapment of heparin within the gelatin structure. The heparin is slowly released in water or blood. This heparin delivery system has been validated.*

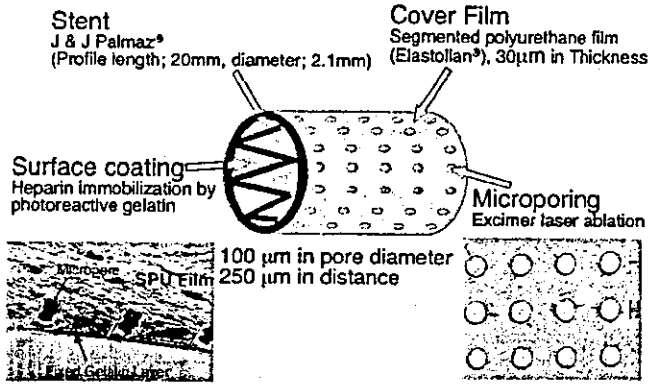

FIGURE 2. *Diagram of preparation of stent grafts with a thin, microporous, SPU film coated with a gelatin layer containing immobilized heparin. Micropores (thickness, 30 μm; pore size, 100 μm; interpore distance, 250 μm) were created in the SPU film with the excimer laser ablation technique. The microporous film was then coated with heparin immobilized in photoreactive gelatin. This treated film covering was rolled on a Palmaz stent and sutured for fixation. Finally, the two ends were glued and attached to each other. Scanning electron microscopy (insets) demonstrated a gelatin layer a few micrometers thick, on the film surface. Micropores were arranged neatly.*

Preparation of Aneurysms in Dogs

Sidewall vein-pouch aneurysms with a 5-mm orifice were constructed bilaterally in the common carotid arteries of seven adult mongrel dogs (weighing 13–15 kg) (12, 19). A total of 13 aneurysms (0.5 cm in diameter at the neck and 1.0 cm in length) were created. Surgical procedures were performed with a protocol approved by our institutional animal care committee. The dogs were maintained with a standard laboratory diet and were treated with 81 mg of aspirin and 100 mg of ticlopidine once daily, beginning 1 week before embolization of the aneurysms. The dogs were anesthetized with an intramuscular injection of Ketalar (50 mg/kg; Parke-Davis, Morris Plains, NJ) and atropine sulfate (0.5 mg), endotracheally intubated, and treated with 20 to 30 mg/kg sodium pentobarbital, administered intravenously. Under sterile condi-

tions in the supine position, the bilateral common carotid arteries and the right external jugular vein were exposed via a 10-cm, cervical, midline, skin incision, with dissection of the muscles and connective tissues. The external jugular vein was isolated and cleared of adventitia. A segment of the vein was tied at both ends with 3-0 silk thread, cut between the threads, removed, flushed with heparinized saline solution, and placed in a bowl of saline solution. The vein specimen was cut into two segments, and one end was firmly tied with 3-0 and 4-0 silk threads. The common carotid arteries were exposed, cleared of adventitia, and isolated between vascular aneurysm clips. A longitudinal, linear, 5-mm arteriotomy, short enough for a saccular aneurysm, was made. The vein graft was then sutured onto the artery (end-to-side anastomosis) with discontinuous 7-0 nylon sutures. After clamp removal, bleeding was controlled with additional suturing or direct compression. The seven dogs each had one aneurysm on each carotid artery (except for one dog in which a single aneurysm was created). The wounds were closed in layers with 3-0 silk sutures. The dogs were then fed and were treated with the same doses of aspirin and ticlopidine. The aneurysms were treated at least 4 weeks after surgery. Aneurysm patency was confirmed before treatment with transfemoral digital subtraction angiography, using a C-arm image intensifier with a neurovascular software supplement (Series 9600; OEC-Diasonics, Salt Lake City, UT).

Aneurysm Embolization

Aneurysms were embolized with the prepared stent grafts 4 to 6 weeks after aneurysm creation, as follows. Each dog underwent general endotracheal anesthesia, and the femoral artery was surgically exposed. An 8-French sheath introducer was inserted into the femoral artery and placed. Then, a 5-French Power Flex PTA balloon catheter (4 or 5 mm in diameter, 2 cm in length, according to the size of the common carotid artery) with the prepared stent graft was inserted through the sheath and advanced across the aneurysm orifice of the carotid artery, with fluoroscopic guidance. The balloon was inflated, and the stent graft was released. Contrast agent injection was performed before and after stent graft implantation, for assessment of the patency of the parent artery and occlusion of the aneurysm. After implantation on both sides, the balloon catheter was removed and the femoral artery was ligated. The postoperative course was uneventful for all dogs.

Histological Processes and Photography

Follow-up carotid artery angiography was performed immediately before killing at predetermined times, i.e., 1 week, 1 month, and 3 months after stenting. Arterial stenosis was defined as the ratio of the stenosis to the normal proximal diameter of the carotid artery. Severe stenosis was defined as an arterial diameter decrease of more than 70%, moderate stenosis as a decrease of 30 to 69%, and mild stenosis as a decrease of 0 to 29%. All aneurysms and adjacent segments of the carotid arteries were removed, fixed in a 10% solution of phosphate-buffered formaldehyde, and embedded in methylmethacrylate. For light microscopy, longitudinal sections (0.5 mm thick) were cut with a circular diamond saw and then hand-polished to a thickness of 30 to 40 μm. The stented aneurysm specimens were prepared for micropathological examinations. After the specimens had been processed and embedded, the paraffin blocks were cut into sections approximately 5 μm thick. One slide from each section was stained with hematoxylin/eosin and Masson's trichrome stain, and a part of each specimen was processed for scanning electron microscopy.

RESULTS

Pilot Study of Appropriate Pore Designs for Covering Films

In our pilot study using heparin-loaded stent grafts (pore diameter, 30 μm; interpore distance, 125 μm) in six dogs, both lateral wall aneurysms created with venous patches and their parent arteries were angiographically patent 2 to 8 weeks after aneurysm production. The aneurysms were embolized at the time of angiography. The parent arteries with the aneurysms were all patent just after embolization and were all occluded 1 month after embolization. Because the area ratio of pores to the film surface had changed from 1.1% (pore size, 30 μm; interpore distance, 125 μm) to 12.6% (pore size, 100 μm; interpore distance, 250 μm), the parent arteries became patent, with aneurysm occlusion, a few months after embolization. The aneurysms became angiographically invisible within a few minutes after embolization.

Surgery

Aneurysms (*Fig. 3*) (n = 13) were successfully constructed on both carotid arteries in all animals, except for one dog in which only one aneurysm was created. All animals recovered from surgery within 4 hours and were used for this study.

Angiographic Findings

Immediately after stent placement, inflow into the aneurysm was almost completely arrested. In a few minutes, all aneurysms became angiographically invisible (*Fig. 4, A* and *B*). At 1 week (*Fig. 4C*), 1 month, and 3 months (*Fig. 5B*) after stent deployment, none of the aneurysms could be identified on angiograms, indicating complete occlusion by the stent grafts. The diameters of the parent vessels were 4 to 5 mm. Mild stenosis was observed in all cases (mean, 5.0%; range, 0–20%; standard deviation,

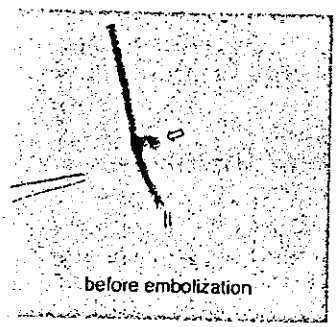

FIGURE 3. *Right carotid artery angiogram obtained just before embolization, demonstrating a broad-necked aneurysm (arrow) with a medial projection.*

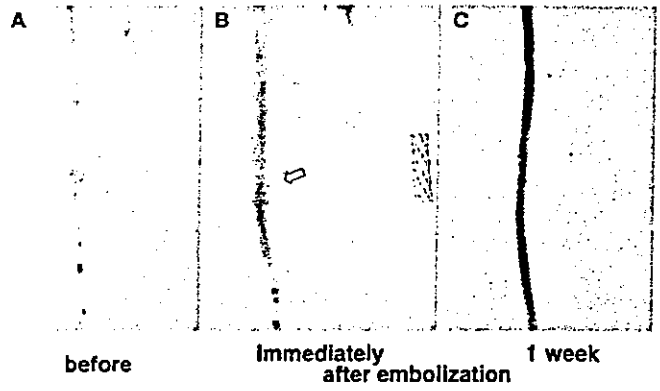

FIGURE 4. *Right carotid artery angiograms obtained before (A), immediately after (B), and 1 week after (C) embolization. The angiograms demonstrated a saccular aneurysm (A), a small residual aneurysm (arrow), which disappeared within a few minutes (B), and a smooth arterial wall, with complete occlusion of the aneurysm (C).*

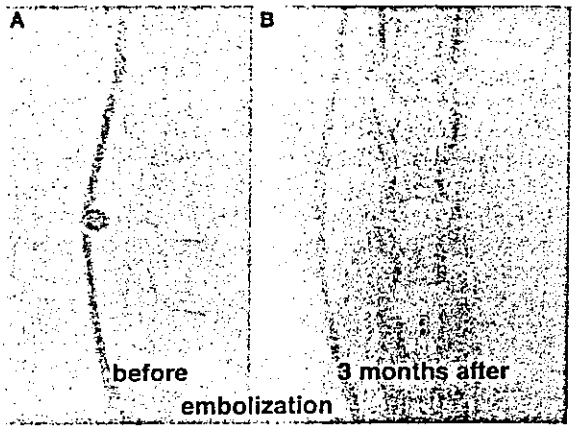

FIGURE 5. *Right carotid artery angiograms obtained before (A) and 3 months after (B) embolization, demonstrating a saccular aneurysm (A) that was completely occluded, leaving sufficient patency of the parent artery (B).*

7.36%) at 1 week, 1 month, and 3 months (*Table 1*). There were no cases of moderate or severe stenosis.

Gross Observations

Soon after stenting, the aneurysms occluded by the stent grafts grossly appeared thrombosed. At 1 week (*Fig. 6*), 1 month, and 3 months after stenting, the aneurysms occluded by the stent grafts were thrombosed and firm in their outward appearance. Even 1 week after stenting, sagittal sections of the specimens demonstrated thin intimal ingrowth via or along the micropores of the stent graft in the carotid artery, on the luminal side of the occluded aneurysms. There was no blood inflow to the aneurysms at any stage.

TABLE 1. Stenosis at 1 week, 1 month, and 3 months after embolization[a]

	Stenosis (%)		
	Mean	Range	SD
1 wk (n = 4)	3.1	0–12.5	6.25
1 mo (n = 3)	9.7	0–20	10.02
3 mo (n = 4)	3.3	0–3.3	6.65
Total	5.0	0–20	7.36

[a] SD, standard deviation. In total, the mean stenosis value was 5.0% (mild).

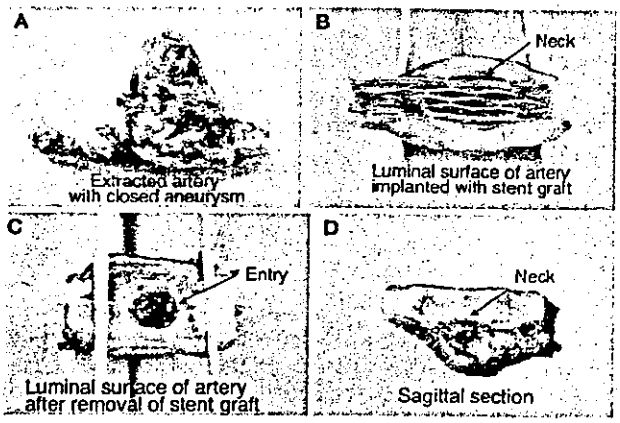

FIGURE 6. *Photographs indicating the gross appearance of the affected carotid artery with an aneurysm, 1 week after stent placement. A, the extracted complex of the affected artery and aneurysm is covered with connective tissue. B, inside the treated area, the stent is associated with the covering film, and no thrombi are evident. A thin intimal fibrocellular layer covers the struts. C and D, the neck of the aneurysm is covered with a thin membrane, perhaps intimal tissue.*

Histopathological Findings

Light microscopic analyses of the specimens removed immediately after implantation of the stent grafts revealed that the neck of the aneurysm was blocked by the stent graft and the aneurysm was also completely packed with thrombus (*Fig. 7*). At 7 days after stent graft implantation, thrombi were observed to occupy each aneurysm cavity (*Fig. 8*). A thin layer of neointima promoted by tissue ingrowth via the micropores covered the in-stent lumen in the early period after placement. The luminal surface of the stent was smooth. Scanning electron microscopy indicated that the luminal surface was covered with confluent endothelial cells (*Fig. 9*). In all of the stented samples, the aneurysms were filled with mature fibrous connective tissue (organized thrombus). A thinner neointima, composed of two to five layers of cells, was present at the neck of the treated lesion in all specimens, except for one

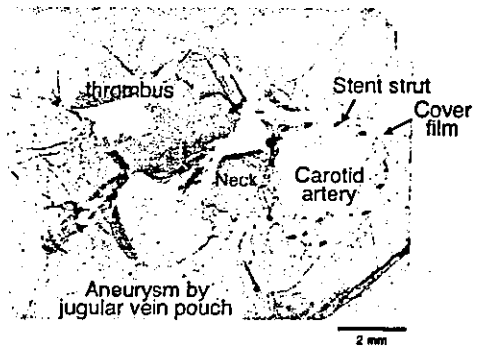

FIGURE 7. *Microscopic view of a transverse section of an embolized aneurysm, immediately after stent graft placement. There is a dumbbell-shaped cavity, of which one part is the created aneurysm and the other is the parent carotid artery. These areas are bordered by part of the expanded stent graft. The stent graft is inside the treated carotid artery. The aneurysm, which was formed with a jugular vein graft, is completely packed with thrombus (original magnification, ×7).*

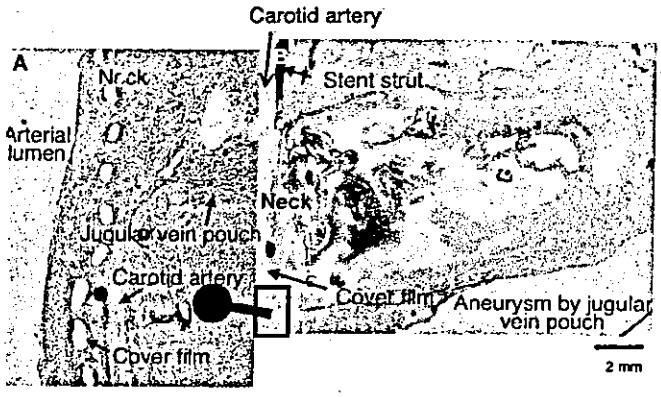

FIGURE 8. *Microscopic views of a sagittal section of an embolized aneurysm 1 week after stent graft placement, under low-power (A) and high-power (B) magnification. The aneurysm is completely packed with old thrombus. There is intimal growth through the micropores into the luminal surface and the aneurysm cavity. The aneurysm is completely occluded by a combination of the mechanical stent graft and biological intima (original magnification, ×5 in A; ×40 in B).*

sample obtained just after stent graft placement. During the process of thrombotic healing, fibrous tissue matures and contracts. Within the fibrous connective tissue (deep to the organized mural thrombus or neointima surrounding the stent struts), there was mild inflammatory cell infiltration involving macrophages, many of which contained hemosiderin.

In specimens obtained 1 or 3 months (*Fig. 10*) after treatment, marked proliferation of granulomatous tissue, containing macrophages, numerous leukocytes, and foreign-body giant cells, was observed. In all stent-treated carotid arteries, the luminal surface of the stent was covered with a thin layer of fibrous tissue and endothelial cells. This tissue layer completely covered the orifice of the aneurysm.

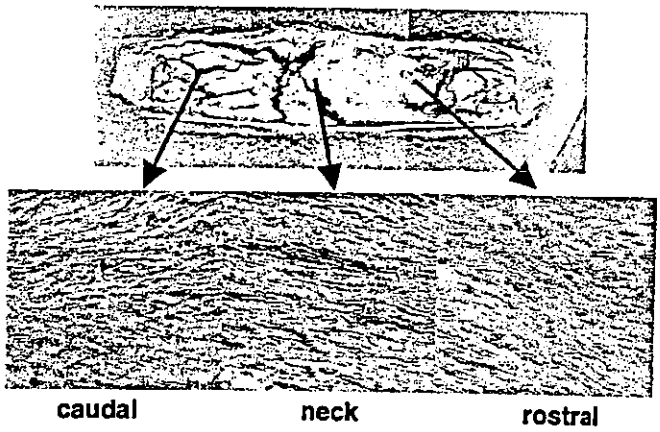

FIGURE 9. *Scanning electron microscopic views of the aneurysm 1 week after stent graft placement, demonstrating the flow-induced macroscopic architectural features of the neointima and the luminal surface covered with confluent endothelial cells in all areas (original magnification,* upper panel, *×400;* lower panel, *×12).*

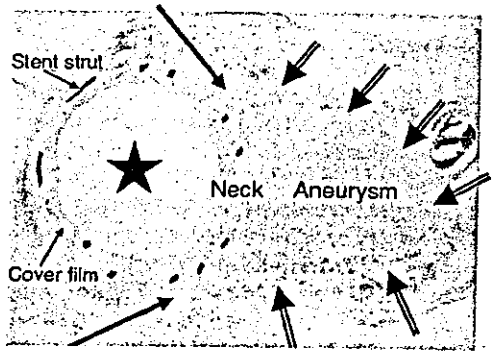

FIGURE 10. *Low-power microscopic view of the aneurysm 3 months after stent graft placement. There is organized thrombus formation within the aneurysm* (open arrows). *The neck of the aneurysm* (solid arrows) *corresponds to the arterial wall defect at the site of anastomosis with the external jugular vein. The parent artery is sufficiently patent* (star) *(hematoxylin and eosin; original magnification, ×5).*

DISCUSSION

Neurointerventions have been commonly performed for treatment of cerebrovascular diseases such as vascular anomalies, aneurysms, and steno-occlusive disease. Stent grafting is an attractive approach for the embolization of aneurysms, because of its time and cost advantages.

The stent graft we developed produced early complete occlusion of experimental aneurysms, without early thrombotic occlusion of the parent carotid artery and with long-term full patency. The graft was developed for the treatment of arterial stenosis. It consists of a balloon-expandable stent with a thin SPU film, onto which micropores are placed with an excimer laser ablation technique (9) and heparin is impregnated with photocured gelatinization (22).

Animal Model of Aneurysms

The most reliable aneurysm model involves end-to-side anastomosis of a venous pouch to the common carotid artery in dogs (12, 13); other methods are time-consuming and have a low rate of reproducibility, although an aneurysm model that mimics the development of human aneurysms has been described (15, 16). In dogs, experiments using different porous or impervious vascular grafts demonstrated that the healing of implanted prostheses approximates human healing, which is much slower than that in other species (such as pigs, calves, and baboons) (30). Studies of interspecies differences in healing responses between dogs and pigs demonstrated that a thicker neointima is formed in pigs, which have a tendency for aneurysm healing, whereas a thin neointima is formed in dogs, which are prone to recurrences after embolization (29). Experiments with a thrombogenic pig model might indicate a higher rate of healing and a scarring response and would be more likely to demonstrate in-stent stenosis than would a canine model. However, the aneurysms might be embolized not only by our stent grafts but also by bare stents, because of the stronger healing mechanism in pigs.

Coils and Their Limitations for Aneurysm Treatment

Intravascular surgery for treatment of intracranial aneurysms is becoming an attractive alternative to conventional surgery, especially since the introduction of Guglielmi electrolytically detachable coils (14, 39). However, coils do not always fill the aneurysm cavity, and additional thrombus formation is necessary to achieve total angiographic occlusion of the aneurysm. Migration and proliferation of VSMCs, with synthesis and deposition of extracellular matrix, are responsible for vessel integrity and vascular repair in the process of wound healing (32, 33). Complete healing of porcine aneurysms is associated with the presence of VSMCs, which form a thick neointima similar to the neointimal hyperplasia that develops after balloon injury. Incomplete healing of aneurysms and recurrences after coil embolization in dogs and rabbits were explained by deficient neointimal formation. Endothelium covering the neck of the aneurysm was not clinically observed until 12 months after Guglielmi detachable coil therapy (3). Endothelialization of the coils may be useful in preventing thromboembolic complications but may also decrease recruitment of VSMCs at the neck of embolized aneurysms. Coils modified with collagen or other growth factors that stimulate fibrosis may have the potential to provide a better framework for fibroblast migration and endothelial cell formation (1).

Stenting for Aneurysm Treatment

To avoid the limitations of coil embolization, endovascular balloon-expandable (2) or self-expanding (10, 11) stent treatment of experimental aneurysms has been reported to be a promising approach. The ability to ablate an aneurysm via an endovascular approach without entering its lumen is an attractive possibility, because the risk of rupturing the aneurysm during packing of the lumen with coils would be avoided. Stenting with a tubular, self-expanding, porous stent produced complete selective occlusion of the aneurysm without penetration of the aneurysmal sac. The endovascular prosthesis, by bridging the aneurysm neck, directs the blood toward the distal part of the parent vessel, which reduces the flow into the aneurysm (blood diversion or channeling effect) and finally promotes occlusion of the aneurysm (40). At sites where the wire crosses a communicating channel, a stent wire not covered by neointima may act as a potential nidus for platelet aggregation. The problem of thromboembolic events resulting from incomplete occlusion remains to be solved. Systemic heparinization prevented thromboembolic events during this embolization procedure. Our heparin-loaded, microporous, stent graft occluded the aneurysms almost instantly and seemed to decrease the formation of distal emboli with continued systemic heparinization. A more precise evaluation of distal emboli remains to be performed. Stenting is, of course, limited by the ability to reach the lesion, and it may not be appropriate in cases in which the aneurysm is located at a bifurcation or has an orifice near arterial branches.

Stent Grafts for Aneurysm Treatment

Bare stents do not cause acute exclusion of the aneurysm lumen from the native vessel lumen. Ideally, stent grafts would be used to immediately exclude aneurysms. There have been reports of the use of stent grafts to exclude broad-neck aneurysms or fistulae from the circulation. A stent graft may be able to close a large orifice and immediately halt blood flow into the aneurysm (8, 25, 38). Prosthetic graft material forms a barrier that is relatively impervious to blood. A stent graft is a prosthetic graft fixed to the arterial wall with an attachment device such as an intravascular stent. The rationale for this technique is that, with isolation of a segment of the artery, the likelihood that intimal hyperplasia will produce restenosis is reduced. In the application of stent grafts to aneurysms, the sizes of the stent and graft are dictated only by the size of the orifice and the diameter of the parent artery and are independent of the size and shape of the aneurysm.

Among 50 patients with peripheral vascular lesions, prosthetic graft incorporation within the wall of the native artery was achieved by establishing a stable flow surface within the lumen of the graft with a modified balloon-expandable Palmaz stent with a knitted Dacron graft (8). The possibility of intimal growth at the ends of the stent was emphasized by a case involving the use of a self-expanding nitinol stent covered with polyester fabric (Craggstent; Mintec, Freeport, Bahamas) for treatment of an iatrogenic pseudoaneurysm of the internal carotid artery (25); such ingrowth could result in stenosis or potential occlusion of the native vessel. The insertion of stents with polyethylacrylate/polymethylmethacrylate covers into the rabbit aorta was accompanied by a strong thrombotic reaction and early occlusion 3 days after deployment, despite sufficient anticoagulant and antiplatelet therapy (intravenous administration of heparin and aspirin). A Dacron-covered niti-

nol stent demonstrated a surprisingly high restenosis rate after 9 months of follow-up monitoring (38). A small arterial diameter and the physical characteristics of the surface, such as roughness, electrical charge, and free surface energy, are important determinants of thrombogenicity (early thrombosis) and tissue incorporation (restenosis) (28).

In normal rabbits, our developed stent graft (produced with a Palmaz-Schatz coronary stent, using the same concept) was used to expand both carotid arteries (each 3 mm in diameter). Heparin-loaded microporous stents were better for prevention of early thrombosis and occlusion and for early induction of endothelialization and prevention of late stenosis with proper control of intimal ingrowth with micropores, compared with the use of bare stents and non-heparin-loaded, microporous, stent grafts. Non-heparin-loaded, microporous, stent grafts tend to result in early occlusion, attributable to hyperthrombogenicity (26).

Before this animal study, we investigated in vitro the expansion characteristics of the stent graft, before and after inflation and subsequent deflation. The fabricated stent graft was easily mounted on a PTA balloon and expanded smoothly with balloon inflation. After balloon deflation, the detached stent graft remained in a fully expanded form, with open-structured micropores on the graft surface (data not shown).

The stent graft we developed demonstrated almost instantaneous occlusion of the aneurysm after deployment and reduced the risk of embolic events because of continuous washout of the produced thrombus. In this study, a control group with bare stents might have been necessary, because bare stents were reported to be effective in producing thrombosis of sidewall aneurysms in canine models (40). A thin layer of neointima, promoted by tissue ingrowth via micropores, covered the in-stent lumen in the early period after placement. In a saccular sidewall aneurysm occlusion model in dogs, the aneurysm orifice was covered with an endothelial layer 21 days after embolization with fibrin glue (36). For an embolization-treated patient with a small internal carotid artery-posterior communicating artery aneurysm, scanning electron microscopy of the aneurysm at 1 month demonstrated endothelial proliferation over the interlocking detachable coils (20). In another study using experimental canine aneurysms, the aneurysm orifices were completely and permanently endothelialized within 1 week after injection of isobutyl cyanoacrylate (41). In this study, the orifice was covered with an endothelial layer as early as 7 days after stent placement. Restoration of the endothelium inhibits the accumulation of smooth muscle cells after denuding arterial injuries (35), and stimulation of endothelial restoration maximizes the regression of intimal hyperplasia (4). Combination therapy with heparin, aspirin, dipyridamole, and dextran was demonstrated to reliably prevent acute thrombotic occlusion of stents in a canine model (28). In another study, the biological effects of engrafted endothelial cells were cell-specific and were superior to the effects of the administration of a single presumptive pharmacological analog of an endothelial product, heparin (25). Endothelial cells secrete heparin-like inhibitors of VSMC proliferation, and experiments involving endothelial denuding have demonstrated that repair of the endothelial cell layer suppresses VSMC growth and prevents intimal thickening (2, 24).

At 1 and 3 months after occlusion of the aneurysms with stent graft implantation, histopathological examinations revealed mature fibrous connective tissue and collagen (indicating well-organized thrombus) filling each aneurysmal lumen and satisfactory patency of the parent carotid arteries, without stenosis. Delayed stenosis was reported at 12 to 18 months after placement of a polyethylene terephthalate endograft in the cervical carotid artery (35). We require a long-term follow-up study, although those results were attributable to the use of a thick nonporous Dacron graft, which was different from our graft with respect to materials, thickness, and pores.

In this study, on the basis of the characteristic features of minimal thrombus formation, rapid control of tissue regeneration, and a role as a physical barrier, our stent grafts were used for embolization of experimental carotid artery aneurysms in dogs. We demonstrated satisfactory occlusion of the aneurysms, together with prevention of early occlusion and maintenance of patency of the parent artery for up to 3 months after implantation, indicating the potential of the stent grafts as an alternative therapeutic device for use in neurosurgery.

CONCLUSION

The stent graft we developed can be considered a promising prosthetic device for embolization of extracranial aneurysms, not only in animal models but also among human patients in the future.

REFERENCES

1. Abrahams JM, Diamond SL, Hurst RW, Zager EL, Grady MS: Topic review: Surface modifications enhancing biological activity of Guglielmi detachable coils in treating intracranial aneurysms. Surg Neurol 54:34–41, 2000.
2. Asahara T, Bauters C, Pastore C, Kearney M, Rossow S, Bunting S, Ferrara N, Symes JF, Isner JM: Local delivery of vascular endothelial growth factor accelerates reendothelialization and attenuates intimal hyperplasia in balloon-injured rat carotid artery. Circulation 91:2793–2801, 1995.
3. Bavinzski G, Talazoglu V, Killer M, Richling B, Gruber A, Gross C, Plenk H: Gross and microscopic findings in aneurysms of the human brain treated with Guglielmi detachable coils. J Neurosurg 91:284–293, 1991.
4. Bjornsson TD, Dryjski M, Tluczek J, Mennie R, Ronan J, Mellin TN, Thomas KA: Acidic fibroblast growth factor promotes vascular repair. Proc Natl Acad Sci U S A 88:8651–8655, 1991.
5. Brilstra EH, Rinkel GJE, Graaf Y, Rooij WJJ, Algra A: Treatment of intracranial aneurysms by embolization with coils: A systematic review. Stroke 30:470–476, 1999.
6. Byrne JV, Sohn M, Molyneux AJ: Five-year experience in using coil embolization for ruptured intracranial aneurysms: Outcomes and incidence of late bleeding. J Neurosurg 90:656–663, 1999.
7. Castaneda F, Ball SM, Wyffels PL, Young K, Li R: Assessment of a polyester-covered nitinol stent in an atherosclerotic swine model. J Vasc Interv Radiol 11:483–491, 2000.
8. Criado E, Marston W, Ligush J, Mauro M, Keagy B: Endovascular repair of peripheral aneurysms, pseudoaneurysms and arteriovenous fistulas. Ann Vasc Surg 11:256–263, 1997.

9. Doi K, Nakayama Y, Matsuda T: Novel compliant and tissue-permeable microporous polyurethane vascular prosthesis fabricated using an excimer laser ablation technique. J Biomed Mater Res 31:27–33, 1996.
10. Geremia G, Brack T, Brennecke L, Haklin M, Falte R: Occlusion of experimentally created fusiform aneurysms with porous metallic stents. AJNR Am J Neuroradiol 21:739–745, 2000.
11. Geremia G, Haklin M, Brennecke L: Embolization of experimentally created aneurysms with intravascular stent devices. AJNR Am J Neuroradiol 15: 1223–1231, 1994.
12. German WJ, Black SPW: Experimental production of carotid aneurysms. N Engl J Med 250:104–106, 1954.
13. Graves VB, Strother CM, Rappe AH: Treatment of experimental canine carotid aneurysms with platinum coils. AJNR Am J Neuroradiol 14:787–793, 1993.
14. Guglielmi G, Viñuela F, Dion J, Duckwiler G: Electrothrombosis of saccular aneurysms via endovascular approach: Part 2—Preliminary clinical experience. J Neurosurg 75:8–14, 1991.
15. Hashimoto N, Handa H, Hazama F: Experimentally induced cerebral aneurysms in rats. Surg Neurol 10:3–8, 1978.
16. Hashimoto N, Kim C, Kikuchi H, Hazama F: Experimental induction of cerebral aneurysms in monkeys. J Neurosurg 67:903–905, 1987.
17. Hietala EM, Salminen US, Stahls A, Valimaa T, Maasilta P, Tormala P, Nieminen MS, Harjula AL: Biodegradation of the copolymeric polylactide stent: Long-term follow-up in a rabbit aorta model. J Vasc Res 38:361–369, 2001.
18. Holmes DR, Camrud AR, Jorgenson MA, Edwards WD, Schwartz RS: Polymeric stenting in the porcine coronary artery model: Differential outcome of exogenous fibrin sleeves versus polyurethane-coated stents. J Am Coll Cardiol 24:525–531, 1994.
19. Kerber AV, Buschman RW: Experimental carotid aneurysms: Part 1—Simple surgical production and radiographic evaluation. Invest Radiol 12:154–157, 1976.
20. Koizumi T, Kawano T, Kazekawa K, Kawaguchi T, Honma T, Kaneko Y, Dosaka A, Tabuchi K: Histological findings in aneurysm treated with IDC: Scanning electron microscopical study. Neurol Surg 25:1027–1031, 1997.
21. Kuether TA, Nesbit GM, Barnwell SL: Clinical and angiographical outcomes, with treatment data, for patients with cerebral aneurysms treated with Guglielmi detachable coils: A single center experience. Neurosurgery 43:1016–1023, 1998.
22. Matsuda T, Nakayama Y: Surface microarchitectural design in biomedical application: In vitro transmural endothelialization on microporous segmented polyurethane films fabricated using an excimer laser. J Biomed Mater Res 31:235–242, 1996.
23. Moret J, Cognard C, Weil A, Castaings L, Rey A: Reconstruction technique in the treatment of wide-neck intracranial aneurysms: Long-term angiographic and clinical results—Apropos of 56 cases. J Neuroradiol 24: 30–44, 1997.
24. Nathan A, Negent MA, Edelman ER: Tissue engineered perivascular endothelial cell implants regulate vascular injury. Proc Natl Acad Sci U S A 92:8130–8134, 1995.
25. Nicholson A, Cook AM, Dyet JF, Galloway JM: Case report: Treatment of a carotid artery pseudoaneurysm with a polyester covered nitinol stent. Clin Radiol 50:872–873, 1995.
26. Nishi S, Nakayana Y, Ueda H, Ishikawa M, Matsuda T: Newly developed stent graft with micropored and heparin impregnated SPU film: Long-term follow-up study in vivo. Interv Neuroradiol 7[Suppl 1]:161–166, 2001.
27. Ozbek C, Heisel A, Gross d, Bay W, Schieffer H: Coronary implantation of silicone-carbide-coated Palmaz-Schatz stents in patients with high risk of stent thrombosis without oral anticoagulation. Cathet Cardiovasc Diagn 41:71–78, 1997.
28. Palmaz JC: Intravascular stents: Tissue-stent interaction and design consideration. Am J Radiol 160:613–618, 1993.
29. Raymond J, Venne D, Allas S, Roy D, Oliva VL, Denbow N, Salazkin I, Lederc G: Healing mechanisms in experimental aneurysms: Part 1—Vascular smooth muscle cells and neointima formation. J Neuroradiol 26:7–20, 1999.
30. Sauvage LR, Berger KE, Wood SJ, Yates SG, Smith JC, Mansfield PB: Interspecies healing of porous arterial prostheses. Arch Surg 109:698–705, 1974.
31. Schellhammer F, Berlis A, Bloss H, Pagenstecher A, Schumacher M: Polylactic acid coating for endovascular stents: Preliminary results in canine experimental arteriovenous fistulae. Invest Radiol 32:180–186, 1997.
32. Schwartz RS, DeBlois D, O'Brian ERM: The intima: Soil for atherosclerosis and restenosis. Circ Res 77:445–465, 1995.
33. Schwartz RS, Edwards WD, Bailey KR, Camrud AR, Jorgenson MA, Holmes DR: Differential neointimal response to coronary artery injury in pigs and dogs. Arterioscler Thromb 14:395–400, 1994.
34. Severini A, Mantero S, Tanzi MC, Cigada A, Salvetti M, Cozzi G, Motta A: Polyurethane-coated, self-expandable biliary stent: An experimental study. Acad Radiol 2:1078–1081, 1995.
35. Smith TP, Alexander MJ, Enterline DS: Delayed stenosis following placement of a polyethylene terephthalate endograft in the cervical carotid artery. J Neurosurg 98:421–425, 2003.
36. Suga T, Sugawara T, Yoshimoto T, Takahashi A: Experimental study of aneurysmal occlusion with fibrin glue. Neurol Surg 20:865–873, 1992.
37. Tamai H, Igaki K, Kyo E, Kosuga K, Kawashima A, Matsui S, Komori H, Tsuji T, Motohara S, Uehata H: Initial and 6-month results of biodegradable poly-L-lactic acid coronary stents in humans. Circulation 102:399–404, 2000.
38. Tepe G, Duda SH, Hanke H, Schulze S, Haigmeier S, Bruck B, Schott U, Betz E, Schmahl F-W, Claussen DC: Covered stents for prevention of restenosis: Experimental and clinical results with different stent designs. Invest Radiol 31:223–229, 1996.
39. Viñuela F, Duckwiler G, Mawad M: Guglielmi detachable coil embolization of acute intracranial aneurysms: Perioperative anatomical and clinical outcome in 403 patients. J Neurosurg 86:475–482, 1997.
40. Wakhloo AK, Schellhammer F, de Vries J, Haberstroh J, Schumacher M: Self-expanding and balloon-expandable stents in the treatment of carotid aneurysms: An experimental study in a canine model. AJNR Am J Neuroradiol 15:493–502, 1994.
41. Zanetti PH, Sherman FE: Experimental evaluation of a tissue adhesive as an agent for the treatment of aneurysms and arterio-venous anomalies. J Neurosurg 36:72–79, 1972.

Acknowledgments

We thank Akio Konishi, Mariko Umeda, and Yoko Goshima for technical assistance. This study was supported by research grants for "Advanced Medical Technology," "Human Genome, Tissue Engineering and Food Biotechnology," and "Aging and Health" and by Cardiovascular Grant 13C-1 from the Ministry of Health, Labour and Welfare of Japan, and by Grant-in-Aid for Scientific Research B2-13450302 from the Ministry of Education, Science, Sports and Culture of Japan.

COMMENTS

The authors demonstrate the usefulness of a novel stent graft for the treatment of experimental carotid aneurysms in a canine model. Only mild (<20%) in-stent stenosis was observed at a 3-month follow-up. The application of covered stents for the treatment of extracranial aneurysms, pseudoaneurysms, and fistulae represents an attractive alternative to currently available techniques. Placement of a covered stent across an aneurysm neck results in the immediate and complete obliteration of the lesion. Other techniques that treat the lesion while preserving the parent vessel (such as stent-supported coiling or stenting alone) may be arduous and complex procedures and may result in subtotal occlusion of the lesion.

To date, the experience with the application of covered stents for the treatment of aneurysms of the extracranial ca-

rotid artery in humans has been disappointing. Smith et al. (1) documented 50 to 100% delayed (12–18 mo) in-stent stenosis in three patients treated with polyethylene terephthalate-coated endografts placed for carotid artery pseudoaneurysms. The current experiments performed with a novel endograft are encouraging, because the data presented suggest that the problem of in-stent stenosis may be reduced or eliminated through the use of a microporous heparin-loaded coating. Further experiments in other animal models and with longer follow-up are warranted to confirm these preliminary results.

David Fiorella
Felipe C. Albuquerque
Phoenix, Arizona

---

1. Smith TP, Alexander MJ, Enterline DS: Delayed stenosis following placement of a polyethylene terephthalate endograft in the cervical carotid artery: Report of three cases. J Neurosurg 98:421–425, 1998.

The authors used heparin-coated covered stents to treat experimental saccular aneurysms in dogs. Angiographic obliteration occurred within minutes after placement of the stents, and the aneurysms remained excluded from the circulation at angiographic follow-up 1 week, 1 month, and 3 months after treatment. Follow-up histological analysis and electron microscopy showed endothelialization of the stent and obliteration of the aneurysm neck. The dog is the most appropriate species for aneurysm modeling. This study was performed well. This strategy for the treatment of aneurysms would be limited to saccular and fusiform aneurysms without important branching vessels and associated with nontortuous parent vessels. Moreover, although good patency rates were achieved with heparin-coated stents in this study, the threat of neointimal hyperplasia and subsequent in-stent stenosis remains. The solution to these limitations may lie in future improvements in stent design and in stents coated with other materials. Despite these limitations, the prospect of using covered stents to treat intracranial aneurysms without the need for embolization of the aneurysm itself is exciting and promising.

Mark R. Harrigan
L. Nelson Hopkins
Buffalo, New York

Covered stents have held promise in the treatment of neurovascular disease for some time but have not gained wide currency, probably because preliminary experience has been plagued by poor patency rates and the development of an exuberant inflammatory response and intimal hyperplasia.

There is considerable excitement in the interventional cardiology community regarding the promising preliminary results with drug-eluting stents in the treatment of coronary stenosis. Specifically, agents that have been shown to inhibit vascular smooth muscle cell proliferation have been used with encouraging results. A number of multicenter clinical trials of drug-eluting stents in the treatment of coronary and peripheral vascular disease are currently ongoing. Outcomes of these trials will most likely have a significant impact on the next generation of stents that are designed specifically for neurovascular, including intracranial, applications.

Nishi et al. have combined in their model features of a covered stent to exclude an aneurysm from the circulation with new drug-loading technology to help maintain patency of the parent vessel. In light of the above-mentioned interventional cardiology literature, one wonders why the authors chose heparin as their drug of choice, rather than the agents currently being investigated that seem to decrease intimal hyperplasia, a cause of recurrent stenosis. Heparin may be helpful in the prevention of acute and subacute thrombosis but probably has no effect on the development of intimal hyperplasia.

For the foreseeable future, the use of stents in the treatment of aneurysms will be limited by the ability to deliver these relatively stiff devices into tortuous vessels. Caging and/or occluding adjacent vessels is an additional problem. Finally, stenosis of the parent vessel secondary to intimal hyperplasia will remain an important concern.

The neurovascular stents of the future not only will be more easily deployed in small, tortuous intracranial vessels but also will probably serve as reservoirs for drugs that will lower the incidence of stenosis and intimal hyperplasia. This report is a small but important step in that direction.

Sean Cullen
Randall T. Higashida
Interventional Neuroradiologists
San Francisco, California

The authors used a new stent graft to treat experimental aneurysms created in the carotid arteries of dogs. The device is novel in that the covering material has pores and is heparin loaded. The device is expected to be able to avoid acute thrombosis and in-stent overgrowth of neointima and therefore would be most beneficial when used in smaller vessels. Variable stent grafts have already been widely used for dissections, aneurysms, and fistulae of large vessels, such as the aorta and its major tributaries, including the extracranial carotid and subclavian arteries. However, for smaller intracranial arteries, tractability (stiffness) and thrombogenicity of the devices will be the major concern. This study is an important approach to make the technology of stent grafting applicable to the neurovascular field. A drawback of this study is that a control study was not performed. Comparison with bare stents or stent grafts with autologous vein grafts or polytetrafluoroethylene, which have been commonly used as covering material, would be important to show the advantages of the new device.

Akiyo Sadato
Nobuo Hashimoto
Kyoto, Japan

Available online at www.sciencedirect.com
SCIENCE DIRECT®
Journal of Controlled Release 89 (2003) 213–224
journal of controlled release
www.elsevier.com/locate/jconrel

Photo-control of the interaction between endothelial cells and photo-cation generatable water-soluble polymers

Yasuhide Nakayama[a,*], Takehisa Matsuda[b,*]

[a]Department of Bioengineering, National Cardiovascular Center Research Institute, 5-7-1 Fujishiro-dai, Suita, Osaka 565-8565, Japan
[b]Department of Biomedical Engineering, Graduate School of Medicine, Kyushu University, 3-1-1 Maidashi, Higashi-ku, Fukuoka 812-8582, Japan

Received 16 October 2002; accepted 16 January 2003

Abstract

In this study photo-control of the non-biospecific interaction between endothelial cell membranes and photo-cation generatable water-soluble polymers were examined. The water-soluble polymers contained triphenylmethane leucohydroxide (malachite green) groups (contents: 0.4 and 1.6 mol%), which dissociate into triphenylmethyl cations and counter hydroxide ions upon ultraviolet light (UV) irradiation, and were prepared by free radical copolymerization of diphenyl(4-vinylphenyl)methane leucohydroxide and acrylamide. The nature and magnitude of the interaction was quantitatively assessed by direct luminescence measurement of the intracellular calcium ion concentration using a calcium-sensitive photoprotein, aequorin. When a PBS buffer of the photoreactive copolymers were added, prior to UV irradiation, to a PBS suspension of cultured bovine endothelial cells loaded with aequorin, no detectable elevation of Ca^{2+} was measured. In contrast, cationic copolymers, derived from the photoreactive copolymers after UV irradiation at a wavelength of $290<\lambda<410$ nm, induced an immediate transient increase in the cytosolic free Ca^{2+} concentration due to a Ca^{2+} inflow from the extracellular space into the cells, which may be due to non-biospecific transmembrane stimulation. Longer UV irradiation exposures of the copolymers and higher concentrations of the polymers, with higher contents of the photodissociable group, resulted in more Ca^{2+} inflow with little cellular damage. The photo-cation generatable copolymers developed here made possible to control the non-biospecific interaction with endothelial cell membranes by UV irradiation condition, and composition and amount of the copolymer.

Keywords: Photo-control; Photo-cation generatable polymer; Malachite green; Cell–polymer interaction; Drug modification

1. Introduction

A variety of proteins with therapeutic value have been modified by covalent attachment to several different water-soluble polymers in an attempt to reduce their immunogenicity in vivo, improve their specific target distribution and improve their blood circulatory lifetime [1–20]. Improvements in the

*Corresponding author. Tel.: +81-6-6833-5012; fax: +81-6-6872-8090.
*Tel.: +81-92-642-6210; fax: +81-92-642-6212.
E-mail addresses: nakayama@ri.ncvc.go.jp (Y. Nakayama), matsuda@med.kyushu-u.ac.jp (T. Matsuda).

0168-3659/03/$ – see front matter
doi:10.1016/S0168-3659(03)00088-9

circulatory lifetime are attributable to an increase in the proteins molecular weight and masking of ligands or antigenic determinants, which are recognized by cellular receptors. Steric hindrance of the proteins antigenic determinants, on the other hand, is believed to reduce the proteins immunogenicity. A number of polymeric modifiers for protein drugs have been examined and include naturally occurring polymers such as proteins(gelatin and albumin) [1,2], polysaccharides (dextran and hyaluranate) [3,4] and nucleic acid (DNA) [5,6], and synthetic polymers such as poly(*N*-vinylpyrrolidone) [7,8], poly(amidoamine) [9], poly(ethylene glycol) (PEG) [10–20] and poly(styrene-co-maleic anhydride) [21]. Currently several PEG-modified proteins are in clinical trials and a number have shown potential for therapeutic use [14–20]. These PEG-modified proteins have been shown to increase blood circulatory time and reduce immunogenicity.

We previously conducted a fundamental and systematic study to determine the nature and magnitude of interaction between bovine aortic endothelial cells (ECs) and various types of water-soluble polymers by means of cytosolic calcium ion mobilization [22]. In the study nonionic polymers, which showed the least affinity for cultured ECs, appeared to be successful in prolonging the blood circulatory lifetime of modified drugs, which were targeted to reside predominantly in blood. In contrast, anionic polymers, which possessed mild affinity for the ECs, showed potential for prolonging the life span of drugs in blood and enhancing their residence on EC membranes. Such attributes were, however, dependent on the degree of interaction between the anionic polymers and ECs. Cationic polymers, on the other hand, were predicted to enhance drug residence on the EC surfaces due to their large stimulation, which may facilitate transmembrane transport of macromolecules. Previously, Hashida and co-workers reported the preparation and evaluation of several conjugates of mitomycin c, an anticancer drug, by modifying the conjugates with electrically charged dextrans and evaluating in vivo the effects of the electric nature of the polymeric modifiers on their disposition characteristics to specified organs [23,24]. From these studies an anionic conjugate was found to persist in blood circulation for long periods and successfully accumulated in the target tumor site after intravenous injection. In contrast, a cationic conjugate showed strong adsorption onto tumor cell surfaces and possessed remarkable antitumor activities after local injection.

In the present study, we report the photo-control of the interaction between photo-cation generatable water-soluble polymers, containing a triphenylmethane leucohydroxide group, and endothelial cells. From this interaction it was anticipated that the design of polymer-modified protein drugs with preferable tissue distribution and localization characteristics could be developed. The nature and magnitude of the interaction was quantitatively assessed by measurement of the concentration of the intracellular free calcium ion, which was inflowed into cells by membrane stimulation. Intracellular calcium ion mobilization, commonly termed the second messenger, is the first sign of various biochemical reactions in cellular systems following external stimulation. Direct measurement of the intracellular calcium ion concentration is achieved by measuring emitted luminescence using a calcium-sensitive photoprotein, aequorin, which binds 3 mol of calcium ion per 1 mol of aequorin [25–28]. The calcium ion bound aequorin complex initially emits blue light before being converted to apoaequorin, which does not bind calcium ions. Thus, aequorin is a useful tool for measurement of the calcium ion concentrations in any system, including cells.

Triphenylmethane leucohydroxide (malachite green) derivatives are well known photochromic molecules, which reversibly dissociate into an ion pair in solution under ultraviolet light (UV) irradiation, producing an intensely deep-green colored triphenylmethyl cation and counter hydroxide ion, according to Scheme 1 [29,30]. Investigations using these derivatives have indicated that the photo-dissociation proceeds very rapidly (within 40 ns) and produces a high quantum yield. It is therefore

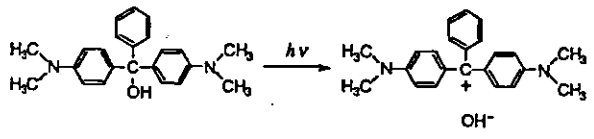

Scheme 1. Chemical reaction in photoinduced dissociation of triphenylmethane leucohydroxide (Malachite green) to triphenylmethyl cation and counter hydroxide ion.

expected that the interaction between water-soluble polymers and endothelial cells could be made photo-controllable by incorporating a photodissociable pendent chromophore, triphenylmethane leucohydroxide into the polymers.

We incorporated a 0.4 and 1.6 mol% triphenylmethane leucohydroxide group into polyacrylamide and evaluated the effect of the photodissociable group on the interaction between the photo-cation generatable water-soluble polymer and endothelial cells.

2. Materials and methods

2.1. Materials

Aequorin, Triton X-100, Trypan blue, 2,2′-azobis(isobutyronitrile) (AIBN), magnesium, iodine and acrylamide were purchased from Wako Pure Chemical Industries (Osaka, Japan). 4-Bromostyrene and 4,4′-bis(dimethylamino)benzophenone were purchased from Aldrich (Milwaukee, WI, USA). Powdered, Ca^{2+}-free, phosphate-buffered saline (PBS(−)) (Nissui Pharmaceutical, Tokyo, Japan) was dissolved in distilled water and adjusted to pH 7.4 at 37 °C. All other regents and solvents were obtained commercially and were purified by distillation.

2.2. Synthesis of diphenyl(4-vinylphenyl)methane leucohydroxide 1 [30]

Magnesium turnings (2.44 g, 0.1 mol) and a trace of solid iodine were added to anhydrous tetrahydrofuran (THF) (20 ml) under a nitrogen atmosphere. The solution was vigorously stirred until the iodine colour disappeared and was then added drop-wise to 4-bromostyrene (18.25 g, 0.1 mol). The mixture was allowed to stand at room temperature for 1 h and then cooled with ice-water. Into the mixture a benzene (500 ml) solution of Michler's ketone (10.94 g, 0.08 mol) was added drop-wise. After stirring for 3 h at room temperature a 10% ammonium chloride solution (50 ml) was added to the reaction mixture. The organic phase was extracted with benzene, dried over anhydrous sodium sulfate and the solvent removed under reduced pressure. The residue was recrystallized three times with methanol; yield of diphenyl(4-vinylphenyl)methane leucohydroxide **1**: 18.5 g (62%); ^{1}H NMR (DMSO-d_6): δ 7.33 (d, J=8.4 Hz, 2H, *m*-H of PhC=C), δ 7.27 (d, J=9.9 Hz, 2H, *o*-H of PhC=C), 7.11 (d, 4H, J=8.7 Hz *o*-H of NPh), δ 6.71 (dd, J=10.8, 18.0 Hz, 1H, PhC*H*=C), δ 6.64 (d, J=8.7 Hz, 4H, *m*-H of NPh), δ 5.77 (d, J=17.1 Hz, 1H, *cis*-H of PhCH=CH_2), δ 5.22 (d, J=10.4 Hz, 1H, *trans*-H of PhCH=CH_2), δ 3.37 (s, 12H, –NCH_3).

2.3. Synthesis of photo-cation generatable water-soluble polymer 2 [30]

A glass tube containing a mixture of acrylamide (2.0 g, 28 mmol) and diphenyl(4-vinylphenyl)methane leucohydroxide **1** (36 mg, 9.7×10^{-2} mmol), 2,2′-azobis(isobtyronitrile) (AIBN, 10 mg, 6.2×10^{-2} mmol; molar ratio of [monomer]/[initiator]=455), and methanol–dimethylsulfoxide (DMSO) (2:1) (3 ml) was sealed by three freeze–pump–thaw cycles under vacuum. Radical polymerization was carried out for 6 h at 60 °C in the dark. The polymer, precipitated by addition of a large amount of methanol, was separated from the solution by filtration. Reprecipitation was carried out from the aqueous solution to the methanol three times. The last precipitation was dried under a vacuum and stored in a dark desiccator. The yield of polymer **2** was 1.9 g (93%). The molecular weight of the polymer was determined by GFC analysis and found to be 78 000. The content of the triphenylmethane leucohydroxide group in the polymer was 0.4 mol%, which was determined from the absorption spectrum using the absorption coefficient of triphenylmethane leucohydroxide which had a maximum absorption at a wavelength of 620 nm in aqueous solution (ε= 6.7×10^4 dm^3 mol^{-1} cm^{-1}).

2.4. General methods

Irradiation was carried out using a 500-W xenon lamp (UXL-500D, Ushio, Tokyo, Japan). The illumination wavelength ($290<\lambda<410$ nm) was selected with the aid of cutoff filters (UV-D25 and UV-31, Toshiba, Tokyo, Japan). The light intensity was measured with a photometer (1.6 mW/cm^2, UVR-1, TOPCON, Tokyo, Japan). The absorption spectra were measured using a Jasco Ubest-30 UV–VIS

spectrophotometer (Japan Spectroscopic, Tokyo, Japan). GFC analysis was carried out on a RI-8012 (TSK_{gel} $G6000PW_{XL}$ and TSK_{gel} $G3000PW_{XL}$; Toso, Tokyo, Japan) after calibration with standard polyethylene glycol samples. The eluent was a PBS(−) solution, pH 7.4. ^1H NMR spectra were obtained on a Jeol JNM-JX-270 (270 MHz) spectrometer (Tokyo, Japan). All ^1H NMR spectra were recorded in DMSO-d_6 solutions using tetramethylsilane as the internal standard.

2.5. Culture of vascular endothelial cells

Bovine aortic endothelial cells (ECs) were isolated from bovine aorta and cultured in Dulbecco's modified Eagle's medium (DMEM) (Flow Laboratories, Irvine, Scotland), supplemented with 15% fetal bovine serum (HyClone Laboratories, Logan, UT, USA) at 37 °C in a water-saturated 5% CO_2–95% air atmosphere. The cells were used for experiments in the eighth to the 14th passage at subconfluence.

2.6. Loading of aequorin into ECs

Loading of aequorin into the ECs was performed by incubating an EC suspension with DMSO using the following procedure [31]. Cultured ECs were dispersed and suspended in 10 ml of PBS(−) containing 1 mM EGTA at 1×10^4 cell/ml. After centrifugation, the cells were resuspended in 90 μl of PBS(−) containing 5 mM EGTA and thereafter 10 μM aequorin was added to the cell suspension. DMSO was added step-wise in 1-μl aliquots over a 9-min period to obtain a cell suspension with a final DMSO concentration of 6%. The suspension was diluted with 10 ml of PBS(−) and centrifuged. After washing and centrifuging twice to remove extracellular aequorin, the cells were resuspended in 10 ml of PBS(−) supplemented with 2 mM $CaCl_2$ and 2 mM $MgCl_2$. The cell suspension was used for measurement of cytosolic calcium ion concentrations within a 2-h period.

2.7. Measurement of cytosolic calcium ion concentration

Investigation of the interaction between polymer 2 and the ECs was quantitatively assessed by measuring changes in the cytosolic free calcium ion concentration [25]. Changes in the intracellular calcium ion concentration were measured using a calcium ion-sensitive photoprotein, aequorin. Binding of calcium ion to aequorin resulted in luminescence changes at a wavelength of 465 nm. The chemiluminescence was measured using a calcium analyzer (CAF-100, Japan Spectroscopic) at 37 °C. The light signals were fed into a personal computer (PC-9801, NEC, Tokyo, Japan) through an analog/digital converter (Canopus, Kobe, Japan) and stored on a hard disk. The intensity of the interaction between polymer 2 and the ECs were evaluated from the relative amount of inflowed calcium ions originated from the transmembrane stimulation with polymer 2, against the total amount of calcium ions that originated from lysis of the cell membranes with 10% Triton X-100. Additional details are described elsewhere in the text.

2.8. Measurement of viability of ECs

EC viability was assessed by the exclusion of trypan blue [32]. ECs (1×10^6 cells) centrifuged were suspended in 100 μl of PBS(−) containing polymer 2 (concentration; 10 mg/ml) and incubated for 10 min. The cell suspension was mixed with 100 μl of PBS(−) of trypan blue (0.4%) at room temperature. After washing and centrifuging twice to remove extracellular trypan blue, the cells were resuspended in 100 μl of PBS(−). About 100 cells were counted using the phase contrast microscopy and cell viability calculated.

3. Results

3.1. Preparation and physical properties of photo-cation generatable water-soluble polymer 2

Photo-cation generatable water-soluble polymer 2 was prepared by free radical copolymerization of acrylamide with the photo-dissociable monomer, diphenyl(4-vinylphenyl)methane leucohydroxide 1, which was synthesized by a Grignard reaction of 4-bromostyrene and Michler's ketone in the dark (Scheme 2). The content of the photodissociable group, triphenylmethane leucohydroxide, in the co-

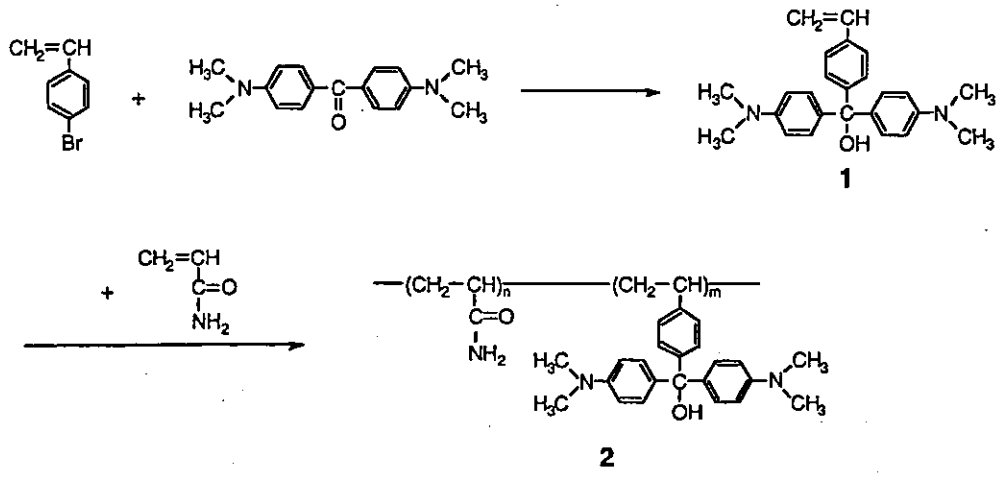

Scheme 2. Reaction scheme of the preparation of photo-cation generatable water-soluble copolymer 2, which is radical copolymer of diphenyl(4-vinylphenyl)methane leucohydroxide 1 and acrylamide.

polymers was determined by absorption spectroscopy using the absorption coefficient of a malachite green carbinol base. Table 1 summarizes the preparation conditions and compositions of the copolymers. The contents of the photodissociable group in the copolymers were 0.4 mol% for copolymer **2a** and 1.6 mol% for copolymer **2b**.

Upon UV irradiation, at a wavelength of $290<\lambda<410$ nm, the aqueous solution of copolymer **2a** (concentration: 2.5 mg/ml) spontaneously turned from colorless to deep-green and exhibited a considerably elevated pH from 6.8 to 8.5 in less than 5 min. In contrast, no change in colour or pH was detected in the absence of copolymer **2** even upon UV irradiation (Fig. 1). The large pH increase was attributed to photo-dissociation of the leucohydroxide group introduced to the copolymer, which generated a triphenylmethyl cation and counter hydroxide ion according to Scheme 1. This change was reversible with the dissociation occurring very rapidly on UV irradiation, whilst the photo-reactive center slowly reverted to the original leucohydroxide species on cessation of the UV irradiation. This

Table 1
Preparation of photo-cation generatable water-soluble polymer 2 and its composition

Copolymer	Feed for 1 (mol%)	M_n[a] (g/mol)	Yield (%)	Content of 1 (mol%)[b]
2a	0.34	78 000	93	0.4
2b	0.69	60 000	17	1.6

[a] Number-average molecular mass determined by GFC (PEO standard).

[b] Determined by absorption spectra at 6.17 nm at pH 3–4.

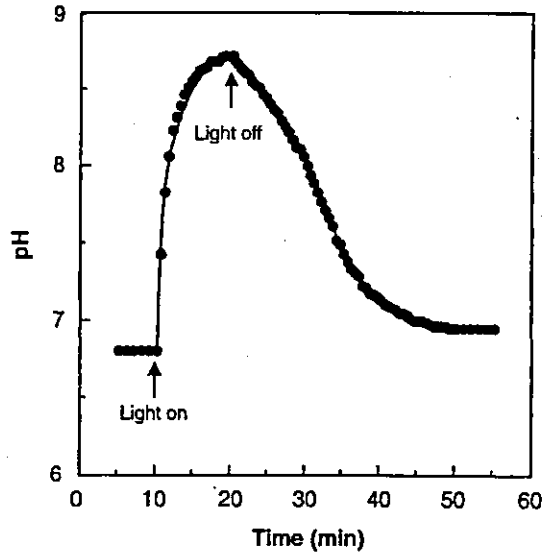

Fig. 1. Photo-induced pH increase of an aqueous solution containing copolymer **2a** (concentration; 2.5 mg/ml). The wavelength of the irradiation was $290<\lambda<410$ nm. pH of an aqueous solution of copolymer **2a** spontaneously elevated from around 6.8 to 8.5 in less than 5 min, which was attributed to photoinduced dissociation of triphenylmethane leucohydroxide introduced in copolymer **2a**.

indicated that positive charges were produced along the polymer chains under UV irradiation.

3.2. Photo-control of the interaction between photo-cation generatable water-soluble polymer 2 and endothelial cells

The nature and magnitude of the interaction between copolymer 2 and the ECs was monitored by measurement of the change in cytosolic calcium ion concentrations using the calcium-sensitive indicator, aequorin. Loading of the aequorin into the ECs was performed as follows [33]. ECs were suspended in a PBS buffer containing 1 mM EGTA at 1×10^4 cells/ml. After loading of the aequorin into the ECs by incubation with DMSO, the ECs were resuspended in a PBS buffer (900 μl) containing 2 mM Ca^{2+} and 2 mM Mg^{2+} in a 2-ml cuvette at 37 °C. After 1 min, luminescence from the loaded aequorin was measured using a luminescence analyzer. Thereafter, a PBS buffer solution (100 μl) of copolymer 2, pre-irradiated with UV light, was added into the cellular suspension. The total amount of luminescence, corresponding to the total amount of aequorin incorporated into the cells, was obtained at the end of the experiment by lysing the cells with a PBS buffer of Triton X-100, which has routinely been used as a membrane protein solubilizer [33]. The resulting light signals were recorded using an analog amplifier and a high-frequency response recorder. The conversion of light signal intensity to calcium ion concentration, $[Ca^{2+}]$, was calculated using the following equation [34]:

$$[Ca^{2+}]\propto L^{1/2.5} \quad (1)$$

where L denotes the light signal intensity of the aequorin luminescence. The amount of calcium ion inflow into the EC cells after stimulation was determined by integration of Eq. (1). The relative amount (%) of inflowed calcium ion ($[Ca^{2+}]_{rel}$), which originated from the cytosol by transmembrane stimulation with copolymer 2, was compared to the total amount of inflowed calcium ions ($[Ca^{2+}]_{total}$), which originated from stimulation with the polymer and Triton X-100, and was defined as follows:

$$[Ca^{2+}]_{rel} = [Ca^{2+}]_{polymer}/[Ca^{2+}]_{total}\times 100 \quad (2)$$

The magnitude of the interaction between copolymer 2 and the ECs was assessed by the amount of $[Ca^{2+}]_{rel}$.

Fig. 2 shows a typical example of the time-dependent changes in chemiluminescence emitted from aequorin-loaded ECs by sequential stimulation with copolymer **2b** at a concentration of 10 mg/ml and then Triton X-100 at 5 min after the polymer addition. Upon the addition of copolymer **2b**, pre-irradiated with UV light, to the suspension of aequorin-loaded ECs the light signal increased transiently without any induction period. No measurable change in the signal was observed by the addition of copolymer 2 without pre-irradiation and even by the elevation of pH to about 9 by the addition of an alkaline solution. The relative amount of inflowed calcium ions, $[Ca^{2+}]_{rel}$, which originated in the cytosol after addition of copolymer **2b** was calculated using Eq. (2) and was found to be 55.5%.

Table 2 summarizes the relative amounts of inflowed calcium ions, $[Ca^{2+}]_{rel}$, generated by the interaction with copolymers **2a** and **2b**. The addition of a PBS buffer of the UV-irradiated copolymers 2 remarkable change in light signal intensity was

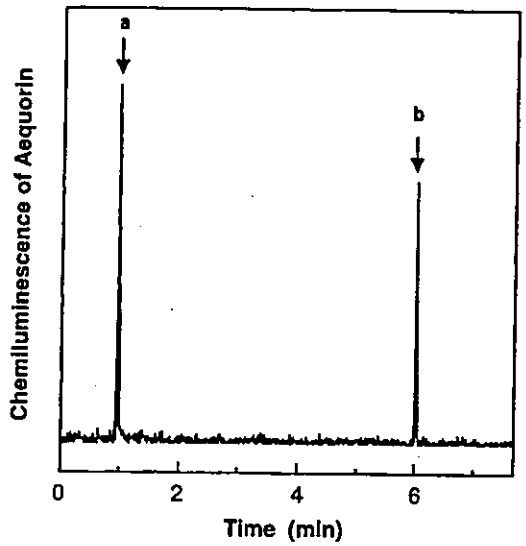

Fig. 2. Chemiluminescence change in a PBS suspension (900 μl) of endothelial cells loaded with aequorin (cell density; 1×10^4 cell/ml). Arrows a and b indicate the times of addition of a PBS solution of copolymer **2b** (100 μl, concentration; 10 mg/ml) preirradiated with UV for 5 min and a PBS solution of Triton X-100 (100 μl, concentration; 10 mg/ml), respectively.

Table 2
Relative amount of calcium ion inflowed into endothelial cells induced by addition of copolymer 2*

Copolymer	Irradiation time (min)	Inflowed $[Ca^{2+}]_{rel}$ (%)
2a	0	0
	5	22.7
2b	0	0
	5	55.5

*One hundred μl of PBS of copolymer 2 (concentration: 10 mg/ml) were added to 900 μl of a PBS suspension of endothelial cells (1×10^5 cells).

observed, resulted in an increase in the cytosolic calcium ion concentration. However, upon addition of a PBS buffer of the non-irradiated copolymer **2** there was no inflow of calcium ions. The change in $[Ca^{2+}]_{rel}$ was enhanced by increasing the content of the photo-dissociable group in the copolymers **2**.

Fig. 3 shows the irradiation time-dependence of cytosolic calcium ion changes induced by copolymer **2a**. The amount of inflowed calcium ions into the ECs increased with increasing pre-irradiation time with copolymer **2a** and remained almost constant (around 20%) after 5 min of irradiation.

The amount of calcium ion inflow could be

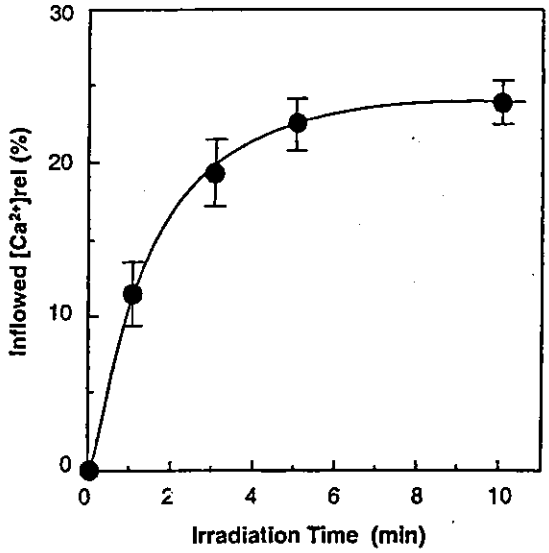

Fig. 3. Change in amount of calcium ions inflowed into endothelial cells suspended in a PBS solution (900 μl) by the addition of a PBS solution of copolymer **2a** (100 μl, concentration; 10 mg/ml) pre-irradiated for ranging from 1 to 10 min ($n=5$).

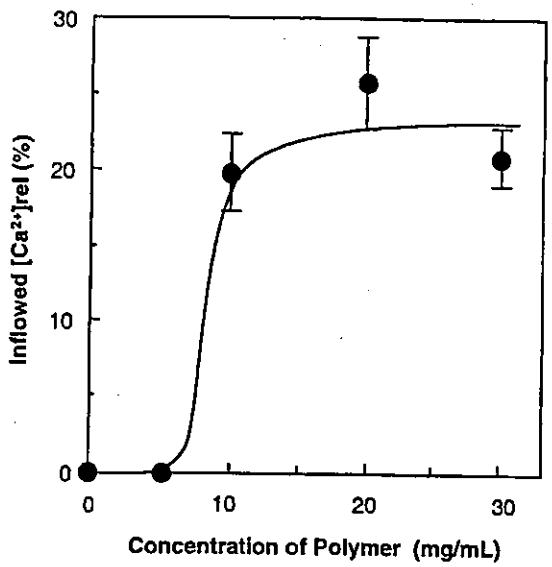

Fig. 4. Concentration-dependent change in amount of inflowed calcium ions into endothelial cells suspended in a PBS solution (900 μl) by the addition of a PBS solution of copolymer **2a** (100 μl), pre-irradiated for 5 min, at the concentration ranging from 0 to 30 mg/ml ($n=5$).

changed by addition of various concentrations of the pre-irradiated copolymer **2a**, as shown in Fig. 4. Upon addition of the polymer solution at the concentration of 5 mg/ml, no inflow of calcium ions was detected, whereas a measurable elevation of $[Ca^{2+}]_{rel}$ was observed for polymer concentrations higher than 10 mg/ml, indicating the presence of threshold in the interaction between cell membranes and the copolymers. The inflowed concentration was almost constant for the polymer concentration range of 10–30 mg/ml.

3.3. Cell viability

The capacity of ECs to exclude trypan blue was tested before and after treatment with copolymer **2a**. Table 3 shows that there was little significant difference between the control and ECs after treatment with copolymer **2a**, regardless of the presence of UV irradiation. These results clearly indicate that treatment of copolymer 2a did not markedly alter the ability of the cells to exclude trypan blue.

To test whether the long-range viability of the cells was affected by treatment with copolymer 2a or

Table 3
Viability of endothelial cells after incubation with copolymer 2 with or without pre-irradiation[a]

	Viability (%)[b]
Control	93.4±14.6
2a without irradiation	87.6±13.9
2a with irradiation	84.5±16.2

[a] Cells were suspended in 100 μl of PBS of copolymer 2a (concentration: 10 mg/ml), pre-irradiated for 5 min and incubated for 5 min.
[b] Measured by trypan blue exclusion method.

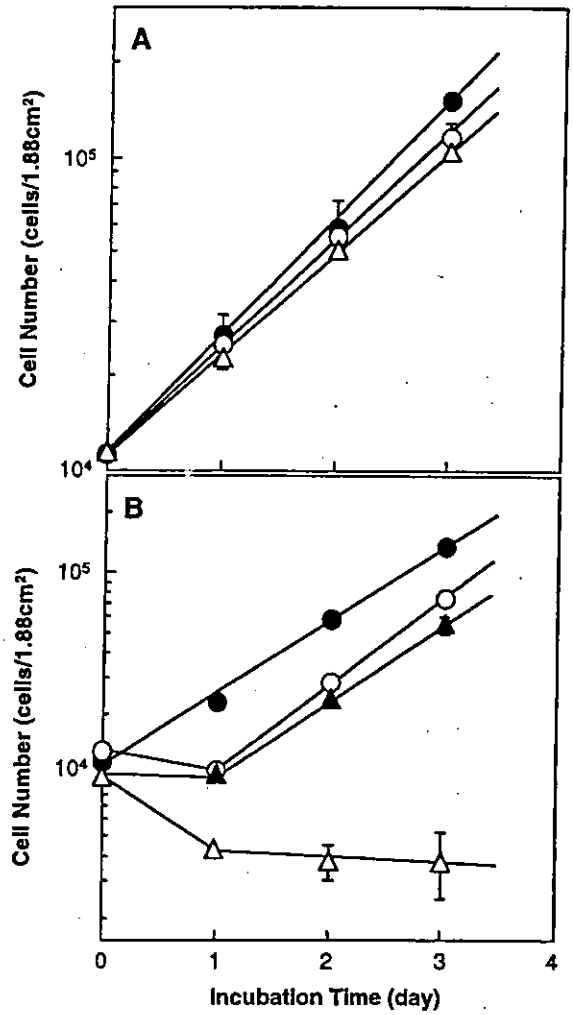

Fig. 5. Cell growth after incubation for 3 min with a PBS solution including copolymer 2a (A, concentration; 0 mg/ml; ●, 1 mg/ml; ○, 10 mg/ml; △) and copolymer 2b (B, concentration; 0 mg/ml; ●, 0.1 mg/ml; ○, 1 mg/ml; ▲, 10 mg/ml; △), both of which were pre-irradiated for 5 min ($n=5$).

2b, monolayered ECs (ca. 1×10^4 cells/well (1.88 cm^2)) were incubated for 3 min at 37 °C with a PBS buffer including pre-irradiated copolymer 2a or 2b. These cells were then placed in a culture medium. Cell growth was observed by harvesting several cultures each day and by measuring any increase in cell numbers. Fig. 5a shows that after treatment with pre-irradiated copolymer 2a, the growth of ECs was no different to that of the control, suggesting that the long-range viability and integrity of the cells were not altered. However, after treatment with copolymer 2b, the growth of the ECs was dose-dependently inhibited (Fig. 5b). Excessive interaction destroyed the membrane integrity, leading to cell death.

4. Discussion

Peptides, enzymes, hormones and other proteins have wide potential for therapeutic applications including thrombolytics, immunomodulators, growth factors, chemotherapeutics and cardiovascular drugs. There are, however, a number of problems associated with the use of protein therapeutics such as their immunogenicity, antigenicity and rapid clearance from blood. To overcome these problems a variety of approaches have been developed. In particular, the advent of recombinant DNA technology has significantly reduced problems associated with immunogenicity and antigenicity of these proteins. However, recombination technology has had little effect on protein stability or improving the drug blood circulating life. Sustained release technologies, such as liposomes and microspheres, have also been developed which allow controlled delivery of drugs to their target and extend their useful time in blood circulation. However, the use of liposomes and microspheres have some disadvantages since they are both rapidly sequestered in the liver, spleen, kidney and reticuloendothelial system and have been shown to act as immunological adjuvants.

A number of chemical modification technologies including succinylation, acylation, guanidation and deamination have been explored. Several polymers have been conjugated to various proteins in an attempt to either increase their blood circulating life and/or reduce immunogenicity [1–21]. One of the most extensively studied modification technologies is